

Nanostructuring of solid surfaces by femtosecond laser pulses

Sergey I. Kudryashov,^a Eugene V. Golosov,^b Andrey A. Ionin,^a
Yuriy R. Kolobov,^b Alexander E. Ligachev,^c Leonid V. Seleznev,^a
Dmitry V. Sinitsyn,^a A.R. Sharipov^a

^a *P.N. Lebedev Physical Institute, Russian Academy of Sciences, Leninsky prospect 53, 119991 Moscow, Russia; phone: +7 (499) 1326739, fax: +7 (499) 7833690, email: sikudr@sci.lebedev.ru.*

^b *Belgorod State University, Belgorod, Russia.*

^c *A.M. Prokhorov General Physics Institute, Moscow, Russia*

Abstract. One-dimensional quasi-periodic structures whose period is much smaller than the wavelength of exciting optical radiation have been obtained on a titanium surface under the multi-shot action of linearly polarized femtosecond laser radiation at various surface energy densities. As the radiation energy density increases, the one-dimensional surface nanogratings oriented perpendicularly to the radiation polarization evolve from quasi-periodic ablative nanogrooves to regular lattices with sub-wavelength periods (90–400 nm). In contrast to the preceding works for various metals, the period of lattices for titanium decreases with increasing energy density. The formation of the indicated surface nanostructures is explained by the interference of the electric fields of incident laser radiation and a surface electromagnetic wave excited by this radiation, as shown by our transient reflectivity measurements and modeling, because the length of the surface electromagnetic wave for titanium with significant interband absorption decreases versus increasing electron excitation of the material.

Keywords: ultrashort laser pulses, titanium, surface nanostructuring, nanogratings, surface electromagnetic waves.

INTRODUCTION

It was recently found that the multi-shot action of femtosecond laser radiation of the visible and near-infrared ranges on the surface of solids makes it possible to reproducibly obtain sub-wavelength (period $\Lambda = 70\text{--}900\text{ nm} \leq \lambda$, where λ is the wavelength of exciting laser radiation) one-dimensional quasi-periodic nanostructures (nanogratings) [1–8]. Such nanogratings on the surfaces of various materials are interesting both because nanoscale periodicity leads to unusual physical or physicochemical properties of a surface continuously varying with Λ [4] and as sources of nanoparticles [1,3–6]. The necessity of the variation of the nanograting period in a wide range by varying the parameters of laser radiation and choosing materials for writing initiates a number of investigations of the effect of the laser polarization (vector e), the wavelength λ and duration of a pulse, the surface energy density F , and the number of acting pulses N on the Λ value [1–8]. In particular, it was found that the wave vector of nanogratings q is always collinear to e and the grating

period Λ increases linearly with λ for femtosecond and short picosecond laser pulses in a limited interval covering the visible and near-infrared ranges [6,7]. At first glance, variations in the parameters F (within several orders of magnitude) [8] and N (within several orders of magnitude) [7] provide wider possibilities of varying Λ . However, the preceding works showed that Λ remains almost unchanged [3,4] or monotonically increases with the surface energy density [5,8], whereas the duration of the irradiation of the surface usually makes it possible only to develop a nanostructure that initially appears on this surface [2,6-7]. The indicated relation between Λ and F hinders the formation of developed one-dimensional nanogratings with minimum possible periods interesting for modern nanotechnologies, because the nanoscale transport of matter decreases sharply at lower energy densities. In view of this circumstance, it is necessary to seek new regimes and materials for the femtosecond laser writing of subwavelength one-dimensional nanogratings that would allow for the efficient creation of one-dimensional surface nanogratings of minimum and maximum sizes.

In this work, sub-wavelength one-dimensional quasi-periodic nanogratings with periods down to 90 nm were written under the action of femtosecond laser pulses with different fluences on a polished surface of chemically pure titanium, which is one of the basic materials of the aerospace industry and implant medicine, and their underlying physical fabrication mechanism was experimentally and theoretically studied.

EXPERIMENTAL

The experiments were performed on an experimental setup including a Ti:sapphire laser (Avesta Project) with fundamental radiation pulses (central wavelength is 744 nm, the FWHM of the lasing band is about 15 nm) with a duration of about 80 fs (FWHM) and an energy of up to 8 mJ [9]. The transverse spatial distribution of the laser field corresponded to the TEM₀₀ mode. Normally, incident laser radiation was focused on a spot with a diameter of 1.2 mm (at a level of $1/e^2$) on the surface of a target (half-bar, a diameter of 8 mm) made from chemically pure, multiply annealed, mechanically polished (rms \leq 50 nm) VT1-0 titanium with a mean grain size of 0.25 μ m (Center for Nanostructure Materials and Technologies, Belgorod State University). The target was placed into a glass cuvette (empty or filled in with a 1-1.5 mm thick layer of doubly-distilled water) on a computer-controlled three-dimensional motorized stage (Fig.1). The energy of laser pulses was varied and controlled by, respectively, a reflecting polarization attenuator (Avesta Project), pyroelectric energymeter (OPHIR) and a DET-210 calibrated photodiode (Thorlab) illuminated by a weak laser beam split through a steering dielectric mirror. The writing of nanostructures was performed by scanning of the titanium target surface with a speed of 20 μ m/s at low laser radiation energies ($<$ 0.5 mJ, peak power $W <$ 4 GW) in order to avoid a noticeable degradation of the energy density distribution on the target surface associated with self-focusing in air (the critical self-focusing power is $W_{cr} \approx$ 3GW [10]) and the accompanying effects of chromatic emission, filamentation, and scattering on a plasma [10,11].

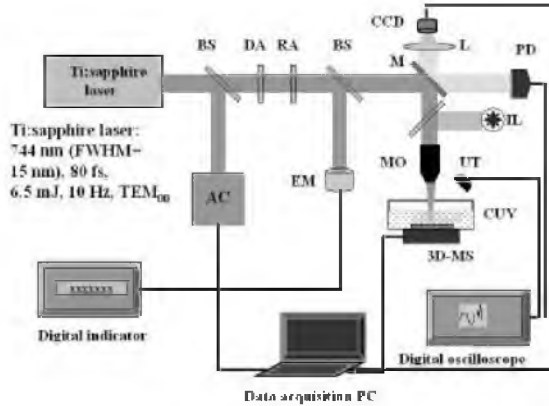


FIGURE 1. Experimental setup for femtosecond laser surface nanostructuring of solids: BS – beam splitter, AC – autocorrelator for laser pulsewidth measurements, DA, RA – variable diffractive and reflective energy attenuators, EM – thermocouple energy meter, M – mirror, L – focusing fused silica lens, CCD – charge-coupled device camera for surface imaging, PD – fast trigger silicon photodiode, IL – illumination lamp, MO – microscope objective, UT – ultrasonic transducer, CUV – glass cuvette with the metallic sample, 3D-MS – three-dimensional motorized micro-stage.

Preliminary characterization of fs laser-fabricated micro-scale surface structures was performed by means of an optical microscope Levenhuk BioView 630 (magnification of 1000 \times), while the final nanoscale topological analysis was done using a scanning electron microscope (SEM) Quanta FEG at magnification up to 100 000 \times .

Probing of transient optical constants of a fs laser-excited titanium was carried out during the fs laser pump pulse measuring its self-reflection in *s*- and *p*-polarizations at an angle of 45 $^\circ$ from titanium foil surface of optical quality at variable F by means of two pyroelectric energymeters.

EXPERIMENTAL RESULTS

During fs laser nanostructuring of titanium surface at $F \approx 17 \text{ mJ/cm}^2$ and $N \approx 500$ we observed well-defined quasi-periodic ($\Lambda \approx 0.4 \text{ }\mu\text{m}$), narrow ($\Delta \leq 0.1 \text{ }\mu\text{m}$) nanotrenches oriented perpendicularly to the laser polarization ($\mathbf{q} \parallel \mathbf{x}, \mathbf{v}, \mathbf{E}$, Fig.2a,3a). This fluence value is close to the multi-shot ($N \approx 500$) nanotrench formation threshold, since such nanotrenches appear irregularly along the scanning path irrespectively the laser energy fluctuations of 5% (Fig.2a). The titanium surface out of the nanotrenches appears unablated, but is heavily contaminated by a residue of ablation products expelled from the trenches (Fig.3a). At higher $F \approx 25\text{-}350 \text{ mJ/cm}^2$ and the same N magnitude well-defined surface nanogratings with $\mathbf{q} \parallel \mathbf{e}, \mathbf{v}$ and sub-wavelength periods within the range $\Lambda \approx 0.2\text{-}0.4 \text{ }\mu\text{m}$ were fabricated (Fig.2b-d,3b-d), while at the increasing fluences a gradual degradation of the grating grooves converting into linear arrays of nanospikes for $F \geq 400 \text{ mJ/cm}^2$ (Fig.2d,3d) was observed. At the intermediate F the fabricated nanogratings exhibit traces of ablation residue (Fig.2b,3b) with their grooves carrying droplet-like nanofragments (Fig.2c,3c),

indicating supercritical thermal, rather than sub-critical thermomechanical spallation origin of the ablation products [12]. As an example, in the former case one can expect condensation of vapor-droplet ablation products upon their hydrodynamic expansion out of the initial narrow nanotrenches (Fig.3a).

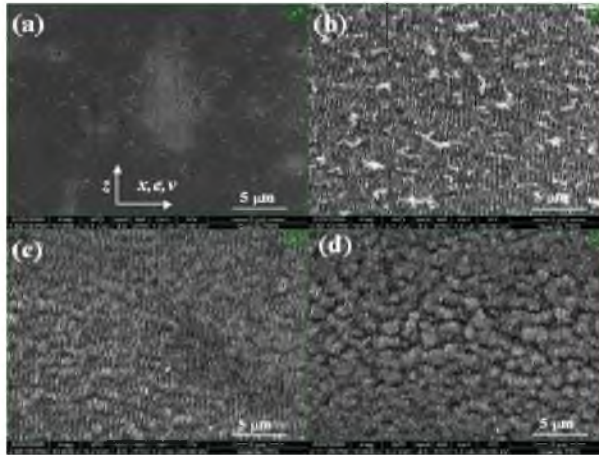


FIGURE 2. Low-magnification ($10\,000\times$) SEM images of titanium surface nanostructured in air at $N \approx 500$ and $F \approx 17$ (a), 25 (b), 100 (c) и 250 (d) mJ/cm^2 .

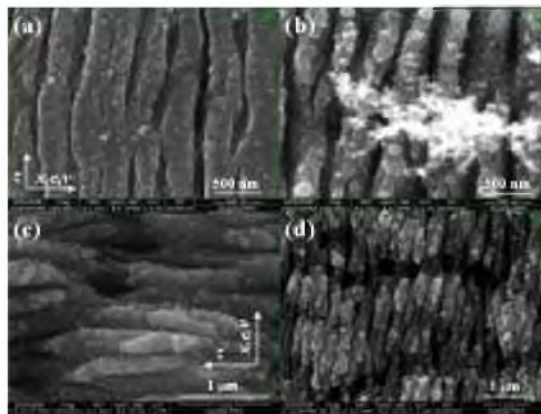


FIGURE 3. High-magnification SEM images of titanium surface nanostructured in air at $N \approx 500$ and $F \approx 17$ (a), 25 (b), 100 (c) и 250 (d) mJ/cm^2 at magnification of $100\,000\times$ (a-c) and $50\,000\times$ (d).

The monotonically decreasing dependence $\Lambda(F)$ (Fig.4) is of particular interest, since it certainly contradicts the results of preceding studies on other metals [3.8]. It is worth noting that the twofold decrease in the period of the nanostructures written on the titanium surface by means of infrared femtosecond laser pulses was previously mentioned in Ref.13, but was referred to two-dimensional nanospike-like structures of

recondensation character and, in the latter case, was attributed to the doubling of the period of dissipative surface nanostructures. In our case, the pronounced orientation of the fabricated surface nanogratings perpendicular to the laser radiation polarization, the quasiperiodicity of the initial nanogrooves (see Figs.2,3), and the high-temperature character of local ablation in nanogrooves in the absence of visible ablation of the material surface itself clearly indicate the local enhancement of the electric field of femtosecond laser radiation on the surface, which is most probable in the case of excitation of surface electromagnetic waves [1,3,5-7,13-14]. More detailed analysis is provided further in Section IV.

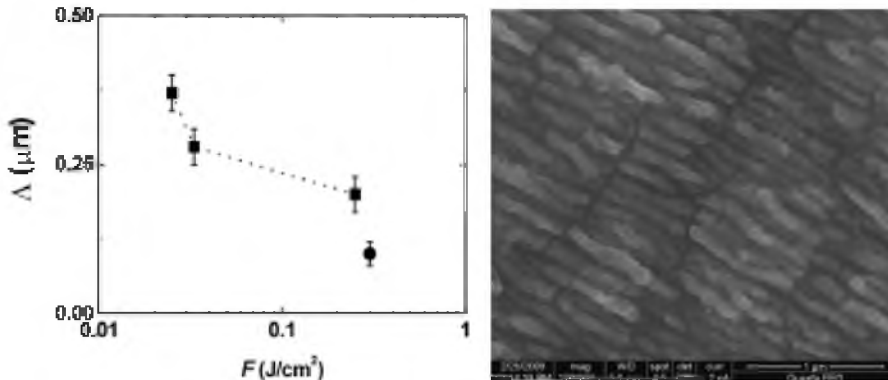


FIGURE 4 (LEFT). Periods Λ of one-dimensional nanogratings on dry (squares) and wet (circles) titanium surfaces versus F at $N \approx 500$.

FIGURE 5 (RIGHT). SEM image of the one-dimensional nanograting with the period $\Lambda \approx 90$ nm written on the wet titanium surface at $F \approx 300$ mJ/cm^2 and $N \approx 500$.

Finally, fs-laser nanostructuring was performed on a wet titanium surface at $F \approx 0.3$ - 0.4 J/cm^2 and $N \approx 500$. In this case, even smaller – by the factor of 2 – one-dimensional nanogratings with $\Lambda \leq 0.1$ μm (Fig.5) were consistently observed in the water environment [9].

DISCUSSION

During our fs-laser nanostructuring studies, the orientation of the one-dimensional surface nanogratings is strictly related to the laser polarization ($\mathbf{q} \parallel \mathbf{e}$) indicating, that the evolution of the surface nanorelief is dictated by some coherent effects of the laser radiation. The main well-known effect is an excitation of a surface electromagnetic (plasmon) wave via scattering of the incident fs laser wave with the wavelength λ on the initial or laser-induced surface nanoroughness, and their constructive interference. As a result, there is a positive feedback for the spatial component of the nanoroughness with wavevector $\mathbf{q} \parallel \mathbf{e}$ and spatial period at the interface with some ambient medium (in this case - air atmosphere, $\epsilon_{1,\text{air}} \approx 1$) [14]

$$A = \lambda \left(\sqrt{\frac{|\epsilon_1|}{|\epsilon_1| - 1}} \pm \sin \theta_{\text{inc}} \right)^{-1} \quad (1),$$

where $|\epsilon_1|$ is the module of the real part of the dielectric function of the laser-excited metal at the laser wavelength. θ_{inc} is the laser angle of incidence (in this work $\theta_{\text{inc}} \approx 0^\circ$). Moreover, according to the previous work [7], upon fs-laser excitation this component of the dielectric function of the metal may vary both in terms of interband and intraband contributions [7]

$$\epsilon_1 = \epsilon_{1,\text{inter}} - \frac{\omega_p^2 \tau_e^2}{1 + \omega^2 \tau_e^2} \quad (2),$$

The latter can change due to 1) decreasing electron relaxation time $\tau_e \propto 1/T_e^2$ resulting from electron heating by the fs-laser pulse to the temperature T_e [15] (the plasma frequency ω_p can rise simultaneously owing to thermal ionization of d -bands [16]); 2) typical reduction of the term $\epsilon_{1,\text{inter}}$ from interband transitions between narrow, high-EDOS d -bands and low-EDOS s,p -bands near the Fermi surface [17]. In the particular case of titanium, however, the interband term predominates in at the laser wavelength over the intraband one (Fig.6), comparing to typical good metals, e.g., copper, silver, gold etc. Nevertheless, detailed understanding of the dielectric function dynamics of titanium during the exciting fs-laser pulse is absent for the reason of its complex band structure [17] and requires direct ultrafast experimental studies of transient optical characteristics of the metal.

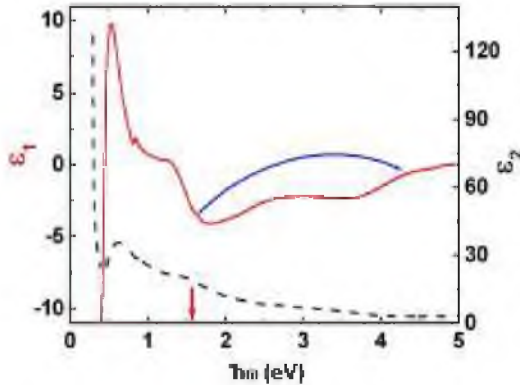


FIGURE 6. Optical spectra of real (ϵ_1 , solid curve) and imaginary (ϵ_2 , dashed curve) parts of dielectric function of titanium (after [18]). The vertical arrow indicates the laser photon energy and the curved blue arrow shows the laser-induced spectral shift.

In this work, probing of transient optical constants of the fs laser-excited titanium carried out during the fs laser pump pulse via measurements of its self-reflection R in s - and p -polarizations at an angle of 45° at variable F demonstrated a consistent decrease of the reflection versus F (Fig.7) starting from the initial values of 0.8 (s -pol.) and 0.4 (p -pol.) with the half-sum of the latter two representing the normal-incidence

reflection (≈ 0.55) of titanium at 744 nm (Fig.8). Therefore, the following decrease of the transient 45° -self-reflection in both these polarizations versus increasing laser fluence down to 0.35 (s-pol.) and 0.15 (p-pol.) at $F \leq 0.3 \text{ J/cm}^2$ may be considered as the corresponding decrease of the normal-incidence reflection to 0.25, which resembles a blue shift of its spectrum by $\leq 3 \text{ eV}$, i.e., $1.6 \text{ eV} + 3 \text{ eV} \leq 4.6 \text{ eV}$ (Fig.8). Such spectral shift of the normal-incidence reflection out of the region of the dominant interband transitions can be related to a transient bleaching of the fs-laser excited material due to a filling of the low-EDOS s,p -bands via photo-induced electron transfer from the high-EDOS d -bands.

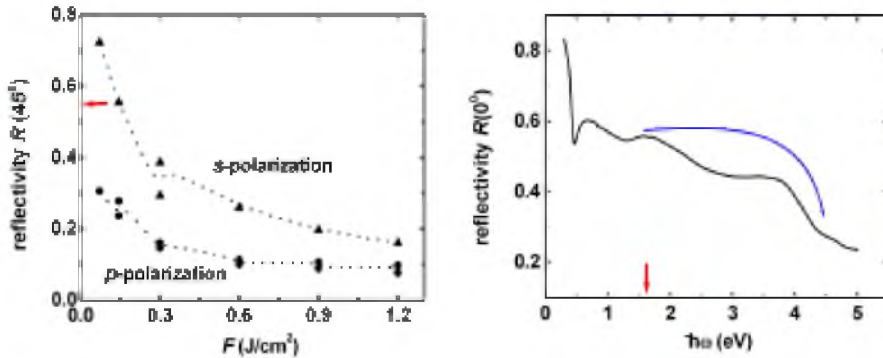


FIGURE 7 (LEFT). Self-reflection of fs-laser pulses at 45° and s,p -polarizations from the titanium surface versus laser fluence F . The horizontal arrow indicates the normal-incidence reflectivity of titanium at the laser photon energy.

FIGURE 8 (RIGHT). Optical spectrum of normal-incidence reflectivity of titanium (after [18]). The vertical arrow indicates the laser photon energy and the curved blue arrow shows the laser-induced spectral shift.

Finally, we have taken some modeling attempts to quantify the experimentally observed spectral shifts increasing as a function of laser fluence, and corresponding spectral variations of the dielectric function of the fs-laser excited titanium (Figs.6,8) to calculate spatial periods Λ of the resulting surface nanogratings by means of Eq.(1). For the different experimental situations of dry clean and oxidized titanium surfaces, and water-titanium interface, the calculated curves $\Lambda(h\omega)$ demonstrate for the increasing spectral shift $\leq 3 \text{ eV}$ a sharp transition from the $0.4\text{-}\mu\text{m}$ initial low- F surface gratings to a large variety of sub- $0.5\text{-}\mu\text{m}$ and much smaller (down to sub100-nm) gratings (Fig.9), while the water environment provides more favorable conditions for fs-laser fabrication of finer nanogratings. The corresponding induced variations of $\varepsilon_1 \approx -(1.1\text{-}1.5)$ exhibit considerable difference regarding the value $\varepsilon_1^0 \approx -3.5$ for the unexcited metal at $\lambda \approx 744 \text{ nm}$ ($n^0 = 2.65$, $k^0 = 3.24$ [18]). These simulation results are consistent with the experimental curve $\Lambda(F)$ in Fig.4, also demonstrating an abrupt decrease of nanograting periods at $F \leq 0.3 \text{ J/cm}^2$.

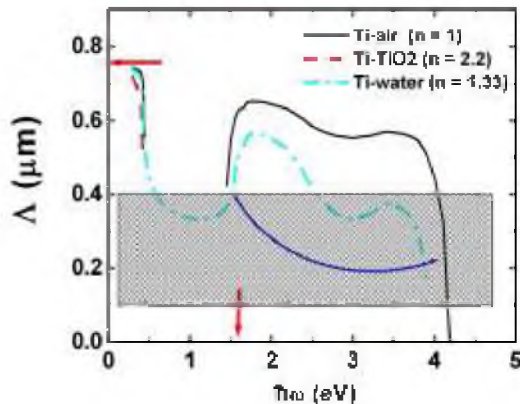


FIGURE 9. Calculated period Λ of one-dimensional nanogratings on dry (black solid line), oxidized (red dashed curve) and wet (blue dash-dot curve) titanium surface versus fs-laser induced spectral shift. The red vertical arrow indicates the laser photon energy, the curved blue arrow shows the laser-induced spectral shift, and the red horizontal arrow shows the laser wavelength.

CONCLUSIONS

In this work, sub-wavelength one-dimensional quasi-periodic nanogratings with periods down to 90 nm were written under the action of femtosecond laser pulses with different fluences on titanium surfaces and their underlying physical fabrication mechanism was experimentally and theoretically studied.

ACKNOWLEDGMENTS

The authors acknowledge a partial support of this work by the Programs of Presidium of RAS, and Russian Foundation for Basic Research within the program of Multi-disciplinary Oriented Fundamental Research (project No. 09-02-12018_OFI-M).

REFERENCES

1. S. V. Zobotnov, L. A. Golovan', I. A. Ostapenko, et al., *JETP Lett.* **83**, 69 (2006).
2. R. Wagner, J. Gottmann, A. Horn, and E. W. Kreutz, *Appl. Surf. Sci.* **252**, 8576 (2006).
3. A. Y. Vorobyev, V. S. Makin, and C. Guo, *J. Appl. Phys.* **101**, 034903 (2007).
4. Y. Yang, J. Yang, C. Liang, and H. Wang, *Opt. Express* **16**, 11259 (2008).
5. G. Miyaji and K. Miyazaki, *Opt. Express* **16**, 16265 (2008).
6. M. Huang, F. Zhao, Y. Cheng, et al., *Opt. Express* **16**, 19354 (2008).
7. M. Huang, F. Zhao, Y. Cheng, et al., *Phys. Rev. B* **79**, 125436 (2009).
8. S. Sakabe, M. Hashida, S. Tokita, et al., *Phys. Rev. B* **79**, 033409 (2009).
9. E.V. Golosov, A. A. Ionin, S. I. Kudryashov et al., *JETP Lett.* **90**, 107 (2009).
10. A. Couairon and A. Mysyrowicz, *Phys. Rep.* **441**, 47 (2007).
11. S. M. Klimentov, T. V. Kononenko, P. A. Pivovarov, et al., *Quantum Electron.* **32**, 433 (2002).
12. S. I. Anisimov and B. S. Luk'yanchuk, *Phys. Usp.* **45**, 293 (2002).

13. V. S. Makin, R. S. Makin, A. Ya. Vorob'ev, and Ch. Guo, *Tech. Phys. Lett.* **34**, 387 (2008).
14. S. A. Akhmanov, V. I. Emel'yanov, N. I. Koroteev, and V. N. Seminogov, *Sov. Phys. Usp.* **28**, 1084 (1985); V.V. Klimov, *Nanoplasmonics*, Fizmatlit, Moscow, 2009.
15. F. Ladstädter, U. Hohenester, P. Puschnig, and C. Ambrosch, *Phys. Rev. B* **70**, 235125 (2004).
16. Z. Lin and L. V. Zhigilei, *Phys. Rev. B* **77**, 075133 (2008).
17. C. K. Sun, F. Vallee, L.H. Acioli, et al., *Phys. Rev. B* **50**, 15337 (1994).
18. E.D. Palik (ed.), *Handbook of Optical Constants of Solids*, Academic Press, Orlando, 1985.